

Makeup-Guided Facial Privacy Protection via Untrained Neural Network Priors

Fahad Shamshad, Muzammal Naseer, and Karthik Nandakumar

Mohamed bin Zayed University of Artificial Intelligence, UAE

Abstract. Deep learning-based face recognition (FR) systems pose significant privacy risks by tracking users without their consent. While adversarial attacks can protect privacy, they often produce visible artifacts compromising user experience. To mitigate this issue, recent facial privacy protection approaches advocate embedding adversarial noise into the natural looking makeup styles. However, these methods require training on large-scale makeup datasets that are not always readily available. In addition, these approaches also suffer from dataset bias. For instance, training on makeup data that predominantly contains female faces could compromise protection efficacy for male faces. To handle these issues, we propose a test-time optimization approach that solely optimizes an untrained neural network to transfer makeup style from a reference to a source image in an adversarial manner. We introduce two key modules: a correspondence module that aligns regions between reference and source images in latent space, and a decoder with conditional makeup layers. The untrained decoder, optimized via carefully designed structural and makeup consistency losses, generates a protected image that resembles the source but incorporates adversarial makeup to deceive FR models. As our approach does not rely on training with makeup face datasets, it avoids potential male/female dataset biases while providing effective protection. We further extend the proposed approach to videos by leveraging on temporal correlations. Experiments on benchmark datasets demonstrate superior performance in face verification and identification tasks and effectiveness against commercial FR systems. Our code and models will be available at <https://github.com/fahadshamshad/deep-facial-privacy-prior>.

Keywords: Facial privacy protection · adversarial makeup transfer · face recognition · black-box attacks

1 Introduction

Face recognition (FR) systems are widely used in various applications, including biometrics [37], security [68], and criminal investigations [49]. The advent of deep learning has significantly improved the performance of FR systems [43,67]. While deep learning-based FR systems offer many potential benefits, they also pose significant privacy risks, enabling potential mass surveillance by governments and private organizations, particularly on social media platforms [1,24,69]. The

Table 1: Comparison of facial privacy protection methods across output naturalness, black-box transferability, verification/identification performance, and unrestricted (semantically meaningful) examples, and use of reference images.

	Adv-Makeup [74]	TIP-IM [72]	AMT-GAN [20]	CLIP2Protect [58]	DFPP (Ours)
Natural outputs	Yes	Partially	Partially	Yes	Yes
Black box	Yes	Yes	Yes	Yes	Yes
Verification	Yes	No	Yes	Yes	Yes
Identification	No	Yes	No	Yes	Yes
Unrestricted	Yes	No	Yes	Yes	Yes
Reference Img.	Yes	No	Yes	No	Yes

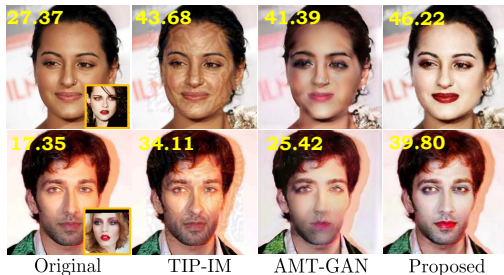


Fig. 1: Our approach generates more natural protected faces for deceiving black-box face recognition systems, outperforming TIP-IM [72] and AMT-GAN [20]. The yellow text at the top-left shows the confidence score (higher is better) from a commercial API when matching the protected image to a false target identity.

prevalence of proprietary, black-box FR models further emphasizes the urgent need for effective facial privacy protection.

Recent studies have explored adversarial attacks to protect facial privacy, but these often struggle to balance naturalness and privacy protection [72]. Noise-based techniques typically produce visible artifacts [71, 73], as shown in Fig. 8. Unrestricted adversarial examples offer better perceptual realism while maintaining privacy [6, 32, 62, 77, 79], with makeup-based methods embedding adversarial perturbations naturally through makeup effects [20, 74]. These methods use generative adversarial networks trained on large makeup datasets to transfer makeup from a reference image to a user’s face, imitating a target identity. Importantly, these makeup-based approaches learn effective *image priors* by capturing natural image statistics from large-scale makeup datasets. Nevertheless, despite their effectiveness, existing adversarial makeup transfer methods suffer from several limitations, as discussed next.

First, training on large makeup datasets is required to capture makeup statistics. These datasets are not only difficult to acquire, but also make these approaches susceptible to dataset bias, as prior information is generally limited to the statistics of the data used for training. **Second**, recent test-time based makeup transfer approaches, such as CLIP2Protect, rely on pre-trained models like StyleGAN for generating protected images. This dependency makes these methods vulnerable to the inherent dataset biases of the pre-trained models, potentially leading to suboptimal performance across diverse demographics. Moreover, high-quality image generators are often hard to train. **Third**, adversarial toxicity can cause false matches in semantic correspondences, leading to unnatural makeup artifacts and changes in the perceived identity of the user

image (see Fig. 8). While some methods use textual makeup guidance, this can be limiting for complex styles, and users may prefer reference images for finer control.

To address these issues, we propose an encoder-decoder-based approach, Deep Facial Privacy Prior (DFPP), that solely optimizes the weights of a randomly initialized neural network at test-time for natural-looking adversarial makeup transfer. Our approach features a **robust correspondence module** for semantic alignment of reference and source images in the encoder’s latent space, and a randomly initialized conditional decoder with **Adaptive Makeup Conditioning** (AMC) layers. We optimize the decoder parameters at test-time to generate protected samples that retain (i) the source’s human-perceived identity, (ii) adopt the reference image’s makeup style, and (iii) mimic the target image identity to evade black-box FR models. To achieve these stated objectives, we carefully designed a composite loss function with three key components: a **Structural Consistency Loss** that maintains source identity via patch-wise matching in a pre-trained ViT feature space; a **Makeup Loss** that facilitates effective makeup transfer by matching region-wise color distribution and global tone while preserving background regions; and an **Adversarial Loss** that ensures the protected sample’s features match the target image in the FR model’s feature space while distancing from the source image embedding.

Unlike recent methods, DFPP avoids the need for large-scale training on makeup datasets, effectively mitigating dataset bias. Extensive experiments in face verification and identification tasks, under both impersonation and dodging scenarios, show that DFPP effectively evades malicious black-box FR models and commercial APIs. Additionally, we demonstrate the effectiveness of DFPP in protecting videos. For videos, we leverage our test-time optimization by transferring weights learned from one frame to subsequent frames, achieving approximately 10 times computational efficiency without compromising privacy.

2 Related Work

Adversarial Examples for Face Recognition Protection: Adversarial attacks have been widely used to protect users from unauthorized FR models. These approaches can be broadly categorized into noise-based and unrestricted adversarial examples. Noise-based methods include data poisoning [9, 60], game theory [40], and privacy masks [80], but often require multiple user images, access to training data, or are limited to white-box settings. Recent work like TIP-IM [72] targets black-box models but produces perceptible noise. Unrestricted Adversarial Examples (UAEs) aim to create less noticeable perturbations [6, 32, 62, 77, 79]. These include patch-based attacks creating wearable items including hats or colorful glasses [29, 61, 71], but they often suffer from poor transferability and unnatural appearance. Generative model-based UAEs show promise but have limited performance in black-box settings [23, 45, 81].

Makeup-based Facial Privacy Protection: Recent approaches have leveraged makeup-based unrestricted attacks [15, 20, 44, 75, 81] to deceive FR systems

by embedding adversarial perturbations into natural makeup effects. However, these methods often require training on large makeup datasets, potentially introducing gender bias, and can produce undesirable artifacts when source and reference styles differ significantly. CLIP2Protect [58] introduced a two-stage, text-guided method to address some of these issues, but it still relied on pre-trained StyleGANs, making it susceptible to inherent dataset biases [25, 38]. Additionally, text-based prompts may not capture complex makeup styles as effectively as reference images. More recently, DiffAM [63] utilized pre-trained diffusion models for facial privacy protection in face verification scenarios, but still relied on a pre-trained generator. In contrast, our proposed approach DFPP eliminates dependency on pre-trained generative models, mitigating dataset bias issues. By employing reference images for makeup style transfer, DFPP offers users enhanced flexibility and granular control over desired makeup styles. Furthermore, we demonstrate the effectiveness of our approach in both verification and identification settings, and extend its application to images and videos.

Untrained Neural Network Priors: While pre-trained generative models have effectively solved a myriad of applications [2, 4, 52–57, 59, 70], untrained neural network priors have also demonstrated significant potential in various vision tasks. These untrained (randomly initialized) neural networks have recently gained traction as effective image priors [46, 66] for a myriad of visual inverse problems, including denoising [36], super-resolution, inpainting [50], image matching [18], enhancement [3, 47, 48, 57] and scene flow [31]. The underpinning idea is that intricate image statistics can be captured by the structure of randomly initialized neural networks, such as CNNs, using the random weights as a parameterization of the resultant output image. While these untrained network priors have found success in various applications [46], their potential in facial privacy protection remains unexplored. In this work, *for the first time* we show how such priors, when paired with our correspondence module and tailored loss functions, can adeptly safeguard user identity through a natural, yet adversarial, makeup transfer using only a source and makeup reference pair.

3 Proposed Methodology

In this section, we first introduce the protection settings and problem formulation, and then elaborate on the proposed method.

3.1 Preliminaries

Protection Settings: Let $\mathbf{x} \in \mathcal{X} \subset \mathbb{R}^n$ represent a face image, with its normalized feature representation extracted by an FR model as $f(\mathbf{x}) : \mathcal{X} \rightarrow \mathbb{R}^d$. We define a distance metric $\mathcal{D}(\mathbf{x}_1, \mathbf{x}_2) = D(f(\mathbf{x}_1), f(\mathbf{x}_2))$ to measure dissimilarity between face images. FR systems operate in *verification* and *identification* modes. In verification, two faces are considered identical if $\mathcal{D}(\mathbf{x}_1, \mathbf{x}_2) \leq \tau$, where τ is the system threshold. In *closed-set* identification, the system compares a probe image to a gallery, identifying the most similar representation. User privacy can

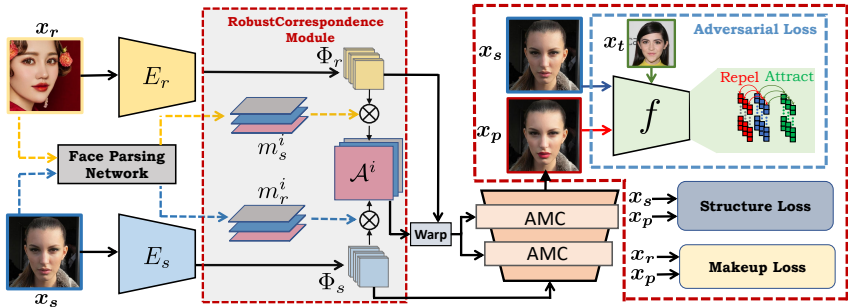


Fig. 2: Pipeline of the Deep Facial Privacy Prior (DFPP) framework: We employ an encoder-decoder architecture with randomly initialized parameters to adversarially transfer makeup from a reference to a source image, guided by our robust correspondence module. The conditional decoder then aligns the source image to match the reference image features via Adaptive Makeup Conditioning (AMC) layers. Notably, the untrained decoder is test-time finetuned using our structured, makeup, and adversarial losses to effectively protect facial privacy.

be protected by deceiving these malicious FR systems through *impersonation* or *dodging* attacks. Impersonation causes false matches with a target identity, while dodging prevents matches with the same person. These attack strategies apply to both verification and identification scenarios. As attackers can exploit both modes using black-box FR models, effective protection strategies must address all these aspects to comprehensively conceal user identity.

Problem Statement: Given a source face image \mathbf{x}_s , our goal is to create a protected face image \mathbf{x}_p that maximizes $\mathcal{D}(\mathbf{x}_p, \mathbf{x}_s)$ for successful dodging and minimizes $\mathcal{D}(\mathbf{x}_p, \mathbf{x}_t)$ for successful impersonation of a target face \mathbf{x}_t , with $\mathcal{O}(\mathbf{x}_s) \neq \mathcal{O}(\mathbf{x}_t)$ where \mathcal{O} provides true identity labels. Concurrently, we aim to minimize $\mathcal{H}(\mathbf{x}_p, \mathbf{x}_s)$, where \mathcal{H} quantifies the degree of unnaturalness introduced in the protected image \mathbf{x}_p . We formulate this as an optimization problem:

$$\min_{\mathbf{x}_p} \mathcal{L}(\mathbf{x}_p) = \mathcal{D}(\mathbf{x}_p, \mathbf{x}_t) - \mathcal{D}(\mathbf{x}_p, \mathbf{x}_s) \text{ s.t. } \mathcal{H}(\mathbf{x}_p, \mathbf{x}_s) \leq \epsilon,$$

where ϵ denotes the bound on the adversarial perturbation. For noise-based approach, $\mathcal{H}(\mathbf{x}_p, \mathbf{x}_s) = \|\mathbf{x}_s - \mathbf{x}_p\|_p$, where $\|\cdot\|_p$ denotes the L_p norm. However, direct enforcement of the perturbation constraint leads to visible artifacts, which affects visual quality and user experience. Constraining the solution search space close to a natural image manifold by imposing an *effective image prior* can produce more realistic images. Note that the distance metric \mathcal{D} is unknown since our goal is to deceive a black-box FR system.

3.2 Deep Facial Privacy Prior (DFPP)

Our method uniquely leverages the neural network’s structure as a prior to generate protected facial images. Unlike previous works that rely on pre-trained models or extensive datasets, we optimize randomly initialized network parameters during inference via gradient descent, capturing an effective facial privacy prior without extensive task-specific training.

Overall Pipeline: As shown in Fig. 2, the DFPP pipeline consists of three key components. First, content encoder E_s and makeup encoder E_r extract multi-scale features from source \mathbf{x}_s and reference \mathbf{x}_r images, respectively. Next, a region-constrained correspondence module establishes semantic correspondences between \mathbf{x}_s and \mathbf{x}_r in deep feature space. Finally, a conditional decoder \mathcal{G} synthesizes the protected image \mathbf{x}_p using multi-scale features from the correspondence module. The randomly initialized decoder network is optimized at test-time using carefully designed identity preservation, makeup transfer, and adversarial losses. DFPP distinguishes itself from existing makeup-based privacy protection methods by leveraging the network structure itself as a prior.

3.2.1 Network Architecture

In this section, we provide details about the architectural components, primarily focusing on the robust correspondence module and the conditional decoder.

Robust Correspondence Module: First, the source \mathbf{x}_s and makeup reference \mathbf{x}_r images are fed into multi-scale feature extractor networks, E_s and E_r , respectively. These networks, pre-trained on ImageNet, extract deep features $\Phi_s = E_s(\mathbf{x}_s)$ and $\Phi_r = E_r(\mathbf{x}_r)$, both represented in $\mathbb{R}^{C \times H \times W}$, which are then reshaped to $\hat{\Phi}_s$ and $\hat{\Phi}_r$ in $\mathbb{R}^{HW \times C}$. These feature maps contain discriminative information representing the semantics of the inputs. A robust correspondence module then computes a dense semantic correspondence matrix $\mathcal{A} \in \mathbb{R}^{HW \times HW}$, which represents how pixels in \mathbf{x}_s are morphed from pixels in \mathbf{x}_r . To avoid artifacts, makeup should be transferred between pixels with similar relative positions (*e.g.*, lips to lips), reflected by high correlation values $\mathcal{A}(u, v)$ between these pixels.

A naive way to find the correlation (attention) matrix is to compare the similarity between the feature maps Φ_s and Φ_r as $\mathcal{A}(u, v) = \frac{\hat{\Phi}_s(u)^T \hat{\Phi}_r(v)}{\|\hat{\Phi}_s(u)\| \|\hat{\Phi}_r(v)\|}$, where $\hat{\Phi}_s(u) \in \mathbb{R}^{C \times 1}$ and $\hat{\Phi}_r(v) \in \mathbb{R}^{C \times 1}$ represent the channel-wise centralized features at position u and v , respectively [16]. Next, the reference features $\hat{\Phi}_r$ are warped to the source features $\hat{\Phi}_s$ according to \mathcal{A} , creating spatially aligned reference-to-source features $\hat{\Phi}_{s \leftarrow r}$ as $\hat{\Phi}_{s \leftarrow r}(u) = \sum_v \text{softmax}(\alpha \mathcal{A}(u, v)) \hat{\Phi}_r(v)$, where α is the temperature parameter to control the sharpness of softmax across v . However, this naive approach often yields poor results due to false matches in semantic correspondence, especially in the presence of adversarial toxicity. In our case, this issue is particularly severe because we only have a single source and reference image to establish correspondence.

To address false matches due to adversarial toxicity, we propose spatially constraining semantic correspondences among facial regions of \mathbf{x}_s and \mathbf{x}_r in deep feature space, using facial parsing masks as guidance. Let m_s^i and m_r^i denote face parsing masks for \mathbf{x}_s and \mathbf{x}_r , where $i \in \text{eye, lip, skin}$. Region-constrained deep features are obtained as $\Phi_s^i = \Phi_s \odot m_s^i$ and $\Phi_r^i = \Phi_r \odot m_r^i$, where \odot is element-wise multiplication. Robust correspondences are established via correlation matrices:

$$\mathcal{A}^i(u, v) = \frac{\hat{\Phi}_s^i(u)^T \hat{\Phi}_r^i(v)}{\|\hat{\Phi}_s^i(u)\| \|\hat{\Phi}_r^i(v)\|}. \quad (1)$$

Using \mathcal{A}^i , we spatially align the region constrained makeup features with the corresponding source features via warping and concatenate them to obtain the final warped features $\hat{\Phi}_s^{conc.}$ after passing through a 1×1 convolution layer.

Conditional Decoder: Guided by the final warped makeup features $\hat{\Phi}_{s \leftarrow r}^{conc.}$ and source features Φ_s , the conditional decoder \mathcal{G}_θ generates protected image \mathbf{x}_p that respects the spatial semantic structure of \mathbf{x}_s and makeup style of \mathbf{x}_r as: $\mathbf{x}_p = \mathcal{G}_\theta(\hat{\Phi}_{s \leftarrow r}^{conc.}, \Phi_s)$. In order to effectively use the warped final makeup features to guide the generation, and to better preserve the makeup style information, we use spatially-adaptive denormalization (SPADE) [42] in \mathcal{G}_θ . Specifically, we progressively inject Φ_s at different scales to modulate the activation functions of the SPADE block in \mathcal{G}_θ . Unlike prior works that employ fixed decoder parameters θ obtained after an intensive training process on a large makeup dataset, we initialize the parameters of the conditional decoder randomly and optimize them during test-time to effectively capture the source-reference pair-specific prior guided by explicit content, makeup, and adversarial objective functions.

3.2.2 Loss Function

Our overall objective function focuses on three critical aspects of the protected image \mathbf{x}_p : the *structure loss* ensures the preservation of the human-perceived identity from \mathbf{x}_s ; the *makeup loss* robustly transfers face makeup of \mathbf{x}_r to the relevant semantic regions of \mathbf{x}_s , and *adversarial loss* generates effective adversarial perturbations to evade black-box FR models.

Structure Loss: Existing makeup transfer methods typically rely on perceptual loss in the VGG feature space to preserve the identity of the source face [39]. However, this loss may suffer from two issues in the presence of adversarial toxicity. *Firstly*, it can cause distortion of the facial attributes of the source image. *Secondly*, a trade-off between preserving the original identity of \mathbf{x}_s and maintaining a high protection success rate may arise due to conflicting objectives. Inspired by recent findings [5, 65] that the deep features in the multi-head self-attention (MSA) layer of the pre-trained DINO-ViT [7] contain crucial structural information, we introduce a loss function that effectively maintains the structural consistency between the \mathbf{x}_s and \mathbf{x}_p . Specifically, we define the structure loss as a difference in self-similarity $S(\cdot)$ of the keys extracted from the attention module at the deepest transformer layer. The structure loss can be expressed as:

$$\mathcal{L}_{\text{struc}}(\mathbf{x}_s, \mathbf{x}_p) = \|S^l(\mathbf{x}_s) - S^l(\mathbf{x}_p)\|_F, \quad (2)$$

where $[S^l(\mathbf{x})]_{i,j} = \cos(k_i^l(\mathbf{x}), k_j^l(\mathbf{x}))$. Here, $k_i^l(\mathbf{x})$ and $k_j^l(\mathbf{x})$ represents i^{th} and j^{th} keys in the l^{th} MSA layer of pre-trained ViT with image \mathbf{x} and ‘cos’ denotes cosine similarity. We apply this loss in a patch-wise contrastive manner [22, 41] to ensure that keys at the same positions have closer distances while maximizing distances between keys at different positions. This approach effectively preserves the source image’s structure (identity) during adversarial optimization.

Robust Makeup Transfer Loss: The primary objective of robust makeup transfer loss is to achieve adversarial makeup transfer between corresponding regions of \mathbf{x}_s and \mathbf{x}_r , while maintaining global coherence and preventing artifacts

in non-makeup areas (*e.g.*, teeth, hair, background). To address challenges posed by adversarial toxicity during optimization, we employ two main components: a ***Histogram Matching Loss*** that matches color histograms in corresponding regions of source and reference makeup images, and a ***Global Loss*** that maintains the overall tone of the reference makeup style.

The ***Histogram Matching*** (HM) Loss applies color histogram matching to corresponding facial regions (skin, lips, and eyes) using face parsing masks. It aims to equalize the color distribution between regions of \mathbf{x}_p and \mathbf{x}_r [14, 30]. Consequently, the HM loss is formulated as the weighted sum of the corresponding local regional losses and can be expressed as $\mathcal{L}_{HM} = \lambda_{\text{lips}}\mathcal{L}_{\text{lips}} + \lambda_{\text{eyes}}\mathcal{L}_{\text{eyes}} + \lambda_{\text{skin}}\mathcal{L}_{\text{skin}}$, where λ_{lips} , λ_{eyes} , and λ_{skin} are hyperparameters. Specifically, each loss item is a local histogram loss, which can be written as:

$$\mathcal{L}_i = \|\mathbf{x}_p \odot m_s^i - \text{HM}(\mathbf{x}_s \odot m_s^i, \mathbf{x}_r \odot m_r^i)\|, \quad (3)$$

where \odot is pixel-wise multiplication, and m_s and m_r are face parsing masks. The resulting histogram-matched regions form a pseudo-ground truth, providing coarse guidance during test-time adversarial optimization. While this discards spatial information, it offers sufficient guidance for makeup color transfer, which is crucial in the presence of adversarial toxicity.

The second component of our robust makeup transfer loss is the ***Global Loss***, which ensures faithful transfer of global makeup elements from \mathbf{x}_r to \mathbf{x}_s . Defined in a patch-wise and multi-scale manner for effective photorealistic transfer, it is expressed as:

$$\mathcal{L}_{\text{glob}} = \sum_l \sum_u \|\Psi((\Phi_{s \leftarrow r}^{\text{conc.}}(u)) - \Psi(\Phi_r(NN(u))))\|_F, \quad (4)$$

where $\Psi(\cdot)$ extracts local patches, and $NN(u)$ is the index of the nearest patch in Φ_r to $\Psi(\Phi_{s \leftarrow r}^{\text{conc.}}(u))$, found using a cross-correlation matrix. This matrix establishes the similarity between patches of source features and makeup face features. Our overall robust makeup loss combines the histogram and global losses: $\mathcal{L}_{\text{makeup}} = \mathcal{L}_{\text{HM}} + \mathcal{L}_{\text{glob}}$.

Adversarial Loss: We optimize the randomly initialized parameters of the untrained conditional decoder \mathcal{G}_θ to find a protected face \mathbf{x}_p whose feature representation is close to the target image \mathbf{x}_t and far from the original image \mathbf{x}_s . This adversarial loss is expressed as:

$$\mathcal{L}_{\text{adv}} = \mathcal{D}(\mathcal{G}_\theta(\Phi_{s \leftarrow r}, \Phi_s), \mathbf{x}_t) - \mathcal{D}(\mathcal{G}_\theta(\Phi_{s \leftarrow r}, \Phi_s), \mathbf{x}_s), \quad (5)$$

where $\mathcal{D}(\mathbf{x}_1, \mathbf{x}_2) = 1 - \cos[f(\mathbf{x}_1), f(\mathbf{x}_2)]$ is the cosine distance. In the black-box setting, we optimize on an ensemble of white-box surrogate models to craft transferable attacks that mimic the unknown FR model’s decision boundary.

Finally, combining all the loss functions, we have $\mathcal{L}_{\text{total}} = \lambda_{\text{struc}}\mathcal{L}_{\text{struc}} + \lambda_{\text{makeup}}\mathcal{L}_{\text{cycle}} + \lambda_{\text{adv}}\mathcal{L}_{\text{adv}}$, where λ terms are hyperparameters. $\mathcal{L}_{\text{struc}}$ preserves the human perceived identity of the image, $\mathcal{L}_{\text{makeup}}$ ensures faithful makeup transfer in relevant regions, and \mathcal{L}_{adv} accounts for the adversarial objective to fool malicious FR models.

4 Experiments

Implementation details: We use the Adam optimizer [28] ($\beta_1 = 0.9$, $\beta_2 = 0.999$, learning rate 2×10^{-4}) for 450 iterations on A100 GPUs. Face parsing is done with BiSeNet [76], followed by mask smoothing to ensure a seamless transition around the edges [35].

Hyperparameters: The components of our loss functions are weighted as follows: structure loss ($\lambda_{\text{ViT}} = 0.001$), makeup loss ($\lambda_{\text{hist}} = 0.8$, $\lambda_{\text{glob}} = 0.2$), and adversarial loss ($\lambda_{\text{adv}} = 0.003$).

Baseline methods: We compare DFPP with recently proposed noise-based and makeup-based privacy protection approaches. Noise-based methods include PGD [34], MI-FGSM [11], TI-DIM [12], and TIP-IM [72], and makeup-based approaches include Adv-Makeup [74] and AMT-GAN [20]. TIP-IM also incorporate multi-target objective in its optimization to find the optimal target image among multiple targets. For fair comparison with AMT-GAN [20], we use TIP-IM’s single-target variant in main experiments. We also present multi-target results to demonstrate DFPP’s effectiveness in such scenarios. In our main experiments, we do not include methods requiring pre-trained high-quality generators like CLIP2Protect [58] and DiffAM¹ [63]. Additionally, CLIP2Protect is text-based, while our approach is image-based, making direct comparison less meaningful. However, we do compare with CLIP2Protect in a separate analysis to demonstrate that DFPP is less gender-biased.

Datasets: For *face verification*, we use CelebA-HQ [27] and LADN [13] for the impersonation attack. We follow the settings of AMT-GAN [20] and select a subset of 1,000 images from CelebA-HQ, reporting average results over the 4 target identities provided by [20]. Similarly, for LADN, we divide the 332 images into 4 groups, where images in each group aim to impersonate the target identities provided by [20]. For the dodging attack, we use CelebA-HQ [27] and LFW datasets [43] by selecting 500 subjects at random, where each subject has a pair of faces. For *face identification*, we use CelebA-HQ [27] and LFW [21] as our evaluation set for both impersonation and dodging attacks. For both datasets, we randomly select 500 subjects, each with a pair of faces. We assign one image in the pair to the gallery set and the other to the probe set. Both impersonation and dodging attacks are performed on the probe set. For impersonation, we insert 4 target identities provided by [20] into the gallery set. For all experiments, we use 10 reference makeup images provided by [20]. Regarding pre-processing, we use MTCNN [78] to detect, crop and align the face image before giving it as input to FR models.

Target Models: We evaluate DFPP’s effectiveness against four black-box FR models: IRSE50 [19], IR152 [10], FaceNet [51], and MobileFace [8]. All input images are pre-processed using MTCNN [78] for face detection and alignment. We also test DFPP against commercial APIs: Face++ and Tencent Yunshentu.

Evaluation metrics: We evaluate DFPP using the Protection Success Rate (PSR) [72], which measures the fraction of protected faces misclassified by FR

¹ The code of DiffAM is not publicly available at the time of submission.

Table 2: Protection success rate (PSR %) of black-box impersonation attack under face verification task where for each column the other three FR models are used as surrogates.

Method	CelebA-HQ				LADN-Dataset				Avg.
	IRSE50	IR152	FaceNet	MobFace	IRSE50	IR152	FaceNet	MobFace	
Clean	7.29	3.80	1.08	12.68	2.71	3.61	0.60	5.11	4.61
PGD [34]	36.87	20.68	1.85	43.99	40.09	19.59	3.82	41.09	25.60
MI-FGSM [11]	45.79	25.03	2.58	45.85	48.90	25.57	6.31	45.01	30.63
TI-DIM [12]	63.63	36.17	15.30	57.12	56.36	34.18	22.11	48.30	41.64
Adv-Makeup [74]	21.95	9.48	1.37	22.00	29.64	10.03	0.97	22.38	14.72
TIP-IM [72]	54.40	37.23	40.74	48.72	65.89	43.57	63.50	46.48	50.06
AMT-GAN [20]	76.96	35.13	16.62	50.71	89.64	49.12	32.13	72.43	52.84
DFPP (Ours)	78.25	41.25	40.86	69.34	90.27	51.66	49.91	77.14	62.34

models, employing thresholding for verification and a closed-set strategy for identification. For face identification, we also use Rank-N Targeted Identity Success Rate (Rank-N-T), indicating the target image appears at least once in the top N gallery candidates, and Rank-N Untargeted Identity Success Rate (Rank-N-U), where the top N candidates exclude the original image’s identity. To assess the realism of protected images, we report FID [17] scores. For commercial APIs, we directly report the confidence scores returned by the respective servers.

4.1 Experimental Results

We generate protected images using three surrogate FR models to mimic the decision boundary of the fourth black-box FR model, employing 10 reference makeup images as per AMT-GAN [20]. For face verification, we set the system threshold at 0.01 false match rate for each FR model: IRSE50 (0.241), IR152 (0.167), MobileFace (0.302), and FaceNet (0.409). Tab. 2

Table 3: Protection success rate (PSR %) of *black-box* dodging (top) and impersonation (bottom) attacks under the face identification task for LFW dataset [21] where for each column the other three FR systems are used as surrogates. R1-U: Rank-1-Untargeted, R5-U: Rank-5-Untargeted, R1-T: Rank-1-Targeted, R5-T: Rank-5-Targeted.

Method	IRSE50		IR152		FaceNet		MobileFace		Average	
	R1-U	R5-U	R1-U	R5-U	R1-U	R5-U	R1-U	R5-U	R1-U	R5-U
MI-FGSM [11]	70.2	42.6	58.4	41.8	59.2	34.0	68.0	47.2	63.9	41.4
TI-DIM [12]	79.0	51.2	67.4	54.0	74.4	52.0	79.2	61.6	75.0	54.7
TIP-IM [72]	81.4	52.2	71.8	54.6	76.0	49.8	82.2	63.0	77.8	54.9
DFPP (Ours)	82.2	55.6	73.0	55.4	80.8	53.4	84.2	66.6	80.05	57.75
	R1-T	R5-T	R1-T	R5-T	R1-T	R5-T	R1-T	R5-T	R1-T	R5-T
MI-FGSM [11]	4.0	10.2	3.2	14.2	9.0	18.8	8.4	22.4	6.15	16.4
TI-DIM [12]	4.0	13.6	7.8	19.6	18.0	32.8	21.6	39.0	12.85	26.25
TIP-IM [72]	8.0	28.2	11.6	31.2	25.2	56.8	34.0	51.4	19.7	41.9
DFPP (Ours)	10.6	33.2	12.8	37.2	26.0	52.8	36.6	58.2	21.50	45.35

presents quantitative results for impersonation attacks in face verification, demonstrating DFPP’s superior performance with average absolute PSR gains of 10% and 12% over AMT-GAN [20] and the noise-based method [72], respectively. The PSR values for dodging and impersonation attacks under the face identification task on the LFW dataset are presented in Tab. 3, where DFPP demonstrates superior performance compared to recent methods at both *Rank-1* and *Rank-5* settings. For this experiment, we randomly select 500 subjects, each having a pair of faces. We assign one image from each pair to the gallery set,

Table 4: FID and PSR comparison. PSR Gain is absolute gain in PSR relative to Adv-Makeup.

Method	FID ↓	PSR Gain ↑
Adv-Makeup [74]	4.23	0
TIP-IM [72]	38.73	35.34
AMT-GAN [20]	34.44	38.12
CLIP2Protect [58]	26.62	50.18
DFPP (Ours)	29.81	47.62

Table 5: PSR comparison on male and female faces (MobileFace as black-box). DFPP provides balanced protection (female/male ratio ≈ 1).

Methods	Images	Male	Female	Ratio
AMT-GAN [20]	1000	511	722	1.41
CLIP2Protect [58]	829	904	722	1.09
Ours	1000	802	817	1.02

and the other to the probe set. Both impersonation and dodging attacks are conducted on the probe set. We excluded AMT-GAN and Adv-Makeup from both tables, as they are specifically trained for the face verification task. Results for dodging attacks under face verification and impersonation attacks under the face identification are provided in the supplementary material. Qualitative results in Fig. 3 also demonstrate DFPP’s superiority in generating realistic protected faces. Unlike TIP-IM’s noise artifacts and AMT-GAN’s unrealistic makeup effects, DFPP produces natural-looking faces that faithfully replicate the reference image’s makeup style.

FID Score: PSR Score: Tab. 4 shows FID scores (lower is better) for makeup-based methods. DFPP achieves lower FID scores and higher PSR than TIP-IM and AMT-GAN, balancing protection and naturalness. While Adv-Makeup has the lowest FID, its PSR is lower due to limited eye-area application. Notably, DFPP’s results are comparable to CLIP2Protect [58], despite the latter’s high-quality pre-trained generator, indicating the strong image prior imposed by untrained neural networks.

Dataset Bias: We evaluate gender bias using 1,000 male and 1,000 female faces from CeleBA-HQ, generating protected faces with DFPP and MobileFace as the black-box model for impersonation in face verification. Tab. 5 shows that, in contrast to AMT-GAN [20] and CLIP2Protect [58], DFPP’s PSR is not significantly affected by gender, providing balanced protection (female/male ratio close to 1) for both male and female faces.

4.2 Effectiveness against Commercial APIs

We evaluate DFPP’s performance against commercial APIs (Face++ and Tencent Yunshentu) in verification mode for

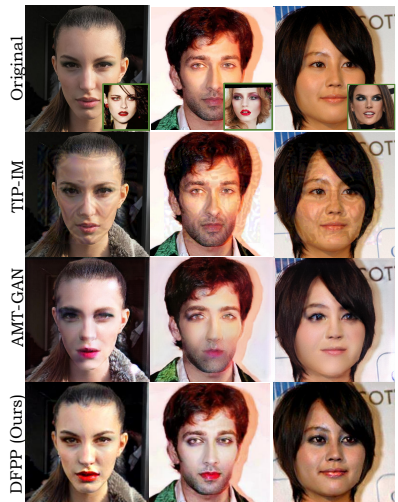


Fig. 3: Qualitative comparison of DFPP with TIP-IM [72] and AMT-GAN [20] approaches. DFPP generates naturalistic images that maintain the human-perceived identity of the original, while faithfully transferring the makeup from the reference image (shown in the top row of the bottom corner).

impersonation. These APIs return confidence scores (0-100) to measure image similarity, with higher scores indicating greater similarity. This test simulates real-world scenarios, as the training data and model parameters of these proprietary FR models are undisclosed. We protect 100 faces from CelebA-HQ using DFPP and baseline methods. Fig. 4 shows the average confidence scores returned by Face++, demonstrating DFPP’s superior PSR compared to baselines. The results for Tencent Yunshentu are provided in the supplementary material.

4.3 Extension to Videos

We extend our approach to videos by leveraging temporal information. Specifically, for each subsequent frame, we initialize the decoder parameters using those optimized for the preceding frame. This strategy provides an advantageous initialization for our optimization, facilitating faster convergence. Evaluations on 10 randomly chosen videos from the RAVDESS dataset [33] indicate that DFPP outperforms AMT-GAN, achieving an absolute improvement of 3.2 in FID score, all the while requiring $10\times$ fewer iterations compared to its image-centric counterpart. Fig. 5 illustrates qualitative results, demonstrating the superior naturalness of our method and the adherence to the reference makeup style.

4.4 Ablation Studies

In this section, we conduct ablation studies to assess the significance of individual components within our overall framework.

Loss functions. We dissect the performance of individual loss components, both qualitatively and quantitatively. The results presented in Fig. 6 highlight the significance of each loss components. Specifically, omitting the histogram loss leads to an imperfect transfer of makeup color from the reference makeup to the source image. On the other hand, the absence of the ViT

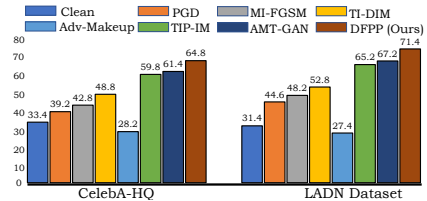


Fig. 4: Average confidence scores (where higher scores are preferable) from commercial API, Face++ for impersonation attacks within the face verification framework. The DFPP method consistently outperforms these approaches.

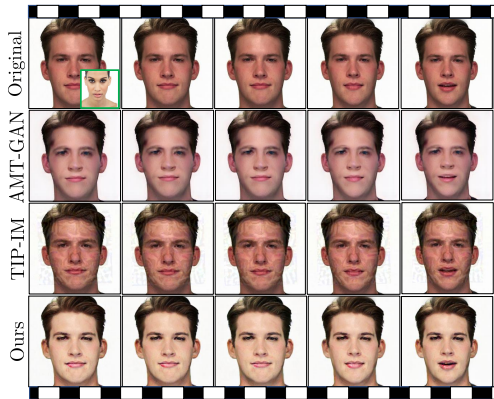


Fig. 5: Qualitative results on videos produced by AMT-GAN [20], TIP-IM [72], and our approach for black-box impersonation attacks in the face verification framework. The reference makeup image is highlighted in the green box. Our approach yields more natural outputs that accurately mimic the makeup style of the reference image.



Fig. 6: Ablation study on histogram and ViT structural losses. Removing the histogram loss results in suboptimal makeup color transfer, while omitting the ViT loss impairs source identity preservation. Our method effectively maintains both the reference makeup style and source identity.

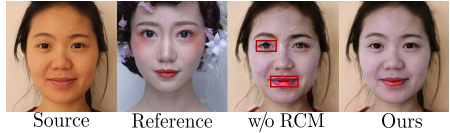


Fig. 7: Ablation for robust correspondence module (RCM). Without RCM, results show makeup artifacts from adversarial toxicity, highlighting the module’s importance in ensuring faithful makeup transfer between corresponding regions of the source and reference images.

Table 6: Quantitative ablative analysis on the histogram, ViT structure, and global losses.

Metrics	w/o $\mathcal{L}_{\text{hist}}$	w/o \mathcal{L}_{ViT}	w/o $\mathcal{L}_{\text{glob}}$	Overall
FID ↓	30.64	30.91	31.07	29.81
PSR ↑	69.31	70.22	69.24	69.34

Table 7: Average PSR of DFPP on CelebA-HQ images with 5 reference makeup images provided by [20]. Std. denotes standard deviation.

	Ref-1	Ref-2	Ref-3	Ref-4	Ref-5	Std. ↓
PSR	62.2	60.4	63.6	66.0	60.8	2.03

structure loss results in a subtle alteration in the identity of the source image compared to when our full objective is employed. We further provide quantitative analysis on the histogram, ViT structure and global loss functions of our proposed approach in Tab. 6. Kindly note that the structure loss helps in maintaining the structural consistency between the source and protected image while histogram and global losses ensure faithful makeup transfer between reference image and the protected sample at the local and global levels respectively. As expected, removing the global loss ($\mathcal{L}_{\text{glob}}$) increases the FID (Tab. 6), verifying its importance in preserving the naturalness of the protected sample.

Robust Correspondence Module: The robust correspondence module (RCM) is crucial for ensuring a faithful makeup transfer between corresponding regions of the source and reference makeup images. As demonstrated in the qualitative results presented in Fig. 7, the absence of the correspondence module leads to makeup artifacts stemming from adversarial toxicity. These artifacts can manifest as misplaced makeup elements or unnatural blending, compromising the overall realism of the protected image. By incorporating the RCM, our approach achieves a more precise and natural-looking makeup transfer, effectively maintaining the identity of the source image while applying the desired makeup style.

Robustness against makeup styles: We also assess the influence of different reference makeup images on the PSR of the resulting output image. We use five reference makeup images to protect 500 CelebA-HQ images with our method. The results in Tab. 7 indicate a slight variation in the PSR (reflected in the low standard deviation) across different makeup reference images, suggesting that DFPP is robust to a range of makeup styles.

On the Role of Makeup:

We further present a visual quality comparison between facial privacy protection methods (DFPP and AMT-GAN) and solely makeup transfer methods like BeautyGAN [30]. As depicted in Fig. 8, BeautyGAN proficiently transfers makeup but falls short in providing protection. In contrast, our method maintains image quality on par with BeautyGAN while achieving a PSR higher than AMT-GAN. This demonstrates DFPP’s ability to strike a crucial balance between aesthetic makeup application and effective privacy protection. The high-quality result highlight the potential of our approach in real-world scenarios where both visual appeal and privacy safeguards are essential.



Fig. 8: Qualitative comparison with BeautyGAN. The red text represents confidence score (higher is better) by a commercial API, when matching the protected image with the false target identity (shown at the bottom of the original image). Note that although BeautyGAN faithfully transfers makeup, it does not offer facial privacy protection.

Table 8: PSR for multi-targets and w/o ensemble (ens.) (Rank-1-Targeted).

Method	ens. 1-target	ens. 4-targets	ens. 10 targets	w/o ens. (10 targets)
TIP-IM	8.0	23.4	69.4	55.4
Ours	10.2	26.6	71.8	58.4

Multi-target setting: Our method adopts the single target and ensemble settings from the recent makeup image-based facial privacy approach [20]. In our main experiments, we showed results with this setting. For TIP-IM, we relied on its official implementation to run the experiments in the AMT-GAN settings (4 FR models, single target, ensemble). Here, we also provide the results in TIP-IM settings that is with multi-target and without ensemble. As depicted in Tab. 8, our DFPP approach consistently outperforms TIP-IM in both multi-target and non-ensemble configurations. This demonstrates the versatility and robustness of DFPP across different operational settings. We deploy IRSE50 as a black-box model, with MobileFace, IR152, and FaceNet acting as surrogates in the ensemble (ens.) setting, and only MobileFace as a surrogate in w/o ensemble setting.

5 Conclusion

To conclude, we propose a test-time optimization approach for facial privacy protection through adversarial makeup transfer. We leverage the structure of the randomly-initialized decoder network as a strong prior, which is fine-tuned through structural and makeup consistency losses to produce a protected sample. The output protected sample is perceptually similar to the source image but contains adversarial makeup of the reference image to evade FR models. Compared to existing baseline methods, our approach offers enhanced naturalness and a superior protection success rate. This adaptability, combined with its ability to function without relying on high-quality pre-trained generative models trained on massive face datasets, makes our approach a promising solution for real-world privacy challenges posed by facial recognition technologies.

References

1. Ahern, S., Eckles, D., Good, N.S., King, S., Naaman, M., Nair, R.: Over-exposed? privacy patterns and considerations in online and mobile photo sharing. In: Proceedings of the SIGCHI conference on Human factors in computing systems. pp. 357–366 (2007) [1](#)
2. Asim, M., Shamshad, F., Ahmed, A.: Blind image deconvolution using pretrained generative priors. arXiv preprint arXiv:1908.07404 (2019) [4](#)
3. Asim, M., Shamshad, F., Ahmed, A.: Patchdip exploiting patch redundancy in deep image prior for denoising. In: NeurIPS 2019 Workshop on Solving Inverse Problems with Deep Networks (2019) [4](#)
4. Asim, M., Shamshad, F., Ahmed, A.: Blind image deconvolution using deep generative priors. IEEE Transactions on Computational Imaging **6**, 1493–1506 (2020) [4](#)
5. Bar-Tal, O., Ofri-Amar, D., Fridman, R., Kasten, Y., Dekel, T.: Text2live: Text-driven layered image and video editing. In: European conference on computer vision. pp. 707–723. Springer (2022) [7](#)
6. Bhattad, A., Chong, M.J., Liang, K., Li, B., Forsyth, D.A.: Unrestricted adversarial examples via semantic manipulation. arXiv preprint arXiv:1904.06347 (2019) [2](#), [3](#)
7. Caron, M., Touvron, H., Misra, I., Jégou, H., Mairal, J., Bojanowski, P., Joulin, A.: Emerging properties in self-supervised vision transformers. In: Proceedings of the IEEE/CVF international conference on computer vision. pp. 9650–9660 (2021) [7](#)
8. Chen, S., Liu, Y., Gao, X., Han, Z.: Mobilefacenets: Efficient cnns for accurate real-time face verification on mobile devices. In: Chinese Conference on Biometric Recognition. pp. 428–438. Springer (2018) [9](#)
9. Cherepanova, V., Goldblum, M., Foley, H., Duan, S., Dickerson, J.P., Taylor, G., Goldstein, T.: Lowkey: Leveraging adversarial attacks to protect social media users from facial recognition. In: International Conference on Learning Representations (2020) [3](#)
10. Deng, J., Guo, J., Xue, N., Zafeiriou, S.: Arcface: Additive angular margin loss for deep face recognition. In: Proceedings of the IEEE/CVF conference on computer vision and pattern recognition. pp. 4690–4699 (2019) [9](#)
11. Dong, Y., Liao, F., Pang, T., Su, H., Zhu, J., Hu, X., Li, J.: Boosting adversarial attacks with momentum. In: Proceedings of the 2018 IEEE/CVF Conference on Computer Vision and Pattern Recognition (CVPR’18). pp. 9185–9193 (2018) [9](#), [10](#)
12. Dong, Y., Pang, T., Su, H., Zhu, J.: Evading defenses to transferable adversarial examples by translation-invariant attacks. In: Proceedings of the 2019 IEEE/CVF Conference on Computer Vision and Pattern Recognition (CVPR’19). pp. 4312–4321 (2019) [9](#), [10](#)
13. Gu, Q., Wang, G., Chiu, M.T., Tai, Y.W., Tang, C.K.: Lادن: Local adversarial disentangling network for facial makeup and de-makeup. In: Proceedings of the IEEE/CVF International Conference on Computer Vision. pp. 10481–10490 (2019) [9](#), [20](#)
14. Gu, S., Bao, J., Yang, H., Chen, D., Wen, F., Yuan, L.: Mask-guided portrait editing with conditional gans. In: Proceedings of the IEEE/CVF conference on computer vision and pattern recognition. pp. 3436–3445 (2019) [8](#)
15. Guetta, N., Shabtai, A., Singh, I., Momiyama, S., Elovici, Y.: Dodging attack using carefully crafted natural makeup. arXiv preprint arXiv:2109.06467 (2021) [3](#)

16. He, M., Chen, D., Liao, J., Sander, P.V., Yuan, L.: Deep exemplar-based colorization. *ACM Transactions on Graphics (TOG)* **37**(4), 1–16 (2018) [6](#)
17. Heusel, M., Ramsauer, H., Unterthiner, T., Nessler, B., Hochreiter, S.: Gans trained by a two time-scale update rule converge to a local nash equilibrium. *Advances in neural information processing systems* **30** (2017) [10](#)
18. Hong, S., Kim, S.: Deep matching prior: Test-time optimization for dense correspondence. In: *Proceedings of the IEEE/CVF International Conference on Computer Vision*. pp. 9907–9917 (2021) [4](#)
19. Hu, J., Shen, L., Sun, G.: Squeeze-and-excitation networks. In: *Proceedings of the IEEE conference on computer vision and pattern recognition*. pp. 7132–7141 (2018) [9](#)
20. Hu, S., Liu, X., Zhang, Y., Li, M., Zhang, L.Y., Jin, H., Wu, L.: Protecting facial privacy: Generating adversarial identity masks via style-robust makeup transfer. In: *Proceedings of the IEEE/CVF Conference on Computer Vision and Pattern Recognition*. pp. 15014–15023 (2022) [2](#), [3](#), [9](#), [10](#), [11](#), [12](#), [13](#), [14](#), [20](#), [22](#)
21. Huang, G.B., Mattar, M., Berg, T., Learned-Miller, E.: Labeled faces in the wild: A database for studying face recognition in unconstrained environments. In: *Workshop on faces in 'Real-Life' Images: detection, alignment, and recognition* (2008) [9](#), [10](#), [20](#), [21](#)
22. Jung, C., Kwon, G., Ye, J.C.: Exploring patch-wise semantic relation for contrastive learning in image-to-image translation tasks. In: *Proceedings of the IEEE/CVF conference on computer vision and pattern recognition*. pp. 18260–18269 (2022) [7](#)
23. Kakizaki, K., Yoshida, K.: Adversarial image translation: Unrestricted adversarial examples in face recognition systems. *arXiv preprint arXiv:1905.03421* (2019) [3](#)
24. Kamgar-Parsi, B., Lawson, W., Kamgar-Parsi, B.: Toward development of a face recognition system for watchlist surveillance. *IEEE Transactions on Pattern Analysis and Machine Intelligence* **33**(10), 1925–1937 (2011) [1](#)
25. Karakas, C.E., Dirik, A., Yalçınkaya, E., Yanardag, P.: Fairstyle: Debiasing stylegan2 with style channel manipulations. In: *European Conference on Computer Vision*. pp. 570–586. Springer (2022) [4](#)
26. Karras, T., Aila, T., Laine, S., Lehtinen, J.: Progressive growing of gans for improved quality, stability, and variation. *arXiv preprint arXiv:1710.10196* (2017) [20](#)
27. Karras, T., Aila, T., Laine, S., Lehtinen, J.: Progressive growing of gans for improved quality, stability, and variation. In: *International Conference on Learning Representations* (2018) [9](#)
28. Kingma, D.P., Ba, J.: Adam: A method for stochastic optimization. *arXiv preprint arXiv:1412.6980* (2014) [9](#)
29. Komkov, S., Petiushko, A.: Advhat: Real-world adversarial attack on arcfac face id system. In: *2020 25th International Conference on Pattern Recognition (ICPR)*. pp. 819–826. IEEE (2021) [3](#)
30. Li, T., Qian, R., Dong, C., Liu, S., Yan, Q., Zhu, W., Lin, L.: Beautygan: Instance-level facial makeup transfer with deep generative adversarial network. In: *Proceedings of the 26th ACM international conference on Multimedia*. pp. 645–653 (2018) [8](#), [14](#)
31. Li, X., Kaesemodel Pontes, J., Lucey, S.: Neural scene flow prior. *Advances in Neural Information Processing Systems* **34**, 7838–7851 (2021) [4](#)
32. Liu, F., Zhang, C., Zhang, H.: Towards transferable unrestricted adversarial examples with minimum changes. *arXiv preprint arXiv:2201.01102* (2022) [2](#), [3](#)
33. Livingstone, S.R., Russo, F.A.: The ryerson audio-visual database of emotional speech and song (ravdess): A dynamic, multimodal set of facial and vocal expressions in north american english. *PLoS one* **13**(5), e0196391 (2018) [12](#)

34. Madry, A., Makelov, A., Schmidt, L., Tsipras, D., Vladu, A.: Towards deep learning models resistant to adversarial attacks. In: Proceedings of the 6th International Conference on Learning Representations (ICLR'18) (2018) **9, 10**
35. Masi, I., Mathai, J., AbdAlmageed, W.: Towards learning structure via consensus for face segmentation and parsing. In: Proceedings of the IEEE/CVF Conference on Computer Vision and Pattern Recognition. pp. 5508–5518 (2020) **9**
36. Mataev, G., Milanfar, P., Elad, M.: Deepred: Deep image prior powered by red. In: Proceedings of the IEEE/CVF International Conference on Computer Vision Workshops. pp. 0–0 (2019) **4**
37. Meden, B., Rot, P., Terhörst, P., Damer, N., Kuijper, A., Scheirer, W.J., Ross, A., Peer, P., Štruc, V.: Privacy-enhancing face biometrics: A comprehensive survey. *IEEE Transactions on Information Forensics and Security* (2021) **1**
38. Muñoz, C., Zannone, S., Mohammed, U., Koshiyama, A.: Uncovering bias in face generation models. arXiv preprint arXiv:2302.11562 (2023) **4**
39. Nguyen, T., Tran, A.T., Hoai, M.: Lipstick ain't enough: beyond color matching for in-the-wild makeup transfer. In: Proceedings of the IEEE/CVF Conference on computer vision and pattern recognition. pp. 13305–13314 (2021) **7**
40. Oh, S.J., Fritz, M., Schiele, B.: Adversarial image perturbation for privacy protection a game theory perspective. In: 2017 IEEE International Conference on Computer Vision (ICCV). pp. 1491–1500. IEEE (2017) **3**
41. Park, T., Efros, A.A., Zhang, R., Zhu, J.Y.: Contrastive learning for unpaired image-to-image translation. In: Computer Vision—ECCV 2020: 16th European Conference, Glasgow, UK, August 23–28, 2020, Proceedings, Part IX 16. pp. 319–345. Springer (2020) **7**
42. Park, T., Liu, M.Y., Wang, T.C., Zhu, J.Y.: Semantic image synthesis with spatially-adaptive normalization. In: Proceedings of the IEEE/CVF conference on computer vision and pattern recognition. pp. 2337–2346 (2019) **7**
43. Parkhi, O., Vedaldi, A., Zisserman, A.: Deep face recognition. In: BMVC 2015—Proceedings of the British Machine Vision Conference 2015. British Machine Vision Association (2015) **1, 9**
44. Pi, J., Zeng, J., Lu, Q., Jiang, N., Wu, H., Zeng, L., Wu, Z.: Adv-eye: A transfer-based natural eye shadow attack on face recognition. *IEEE Access* (2023) **3**
45. Poursaeed, O., Jiang, T., Yang, H., Belongie, S., Lim, S.N.: Robustness and generalization via generative adversarial training. In: Proceedings of the IEEE/CVF International Conference on Computer Vision. pp. 15711–15720 (2021) **3**
46. Qayyum, A., Ilahi, I., Shamshad, F., Boussaid, F., Bennamoun, M., Qadir, J.: Untrained neural network priors for inverse imaging problems: A survey. *IEEE Transactions on Pattern Analysis and Machine Intelligence* (2022) **4**
47. Qayyum, A., Sultani, W., Shamshad, F., Qadir, J., Tufail, R.: Single-shot retinal image enhancement using deep image priors. In: Medical Image Computing and Computer Assisted Intervention—MICCAI 2020: 23rd International Conference, Lima, Peru, October 4–8, 2020, Proceedings, Part V 23. pp. 636–646. Springer (2020) **4**
48. Qayyum, A., Sultani, W., Shamshad, F., Tufail, R., Qadir, J.: Single-shot retinal image enhancement using untrained and pretrained neural networks priors integrated with analytical image priors. *Computers in Biology and Medicine* **148**, 105879 (2022) **4**
49. Rezende, I.N.: Facial recognition in police hands: Assessing the 'clearview case' from a european perspective. *New Journal of European Criminal Law* **11**(3), 375–389 (2020) **1**

50. Schrader, K., Alt, T., Weickert, J., Ertel, M.: Cnn-based euler’s elastica inpainting with deep energy and deep image prior. In: 2022 10th European Workshop on Visual Information Processing (EUVIP). pp. 1–6. IEEE (2022) [4](#)
51. Schroff, F., Kalenichenko, D., Philbin, J.: Facenet: A unified embedding for face recognition and clustering. In: Proceedings of the IEEE conference on computer vision and pattern recognition. pp. 815–823 (2015) [9](#)
52. Shamshad, F., Abbas, F., Ahmed, A.: Deep ptych: Subsampled fourier ptychography using generative priors. In: ICASSP 2019-2019 IEEE International Conference on Acoustics, Speech and Signal Processing (ICASSP). pp. 7720–7724. IEEE (2019) [4](#)
53. Shamshad, F., Ahmed, A.: Robust compressive phase retrieval via deep generative priors. arXiv preprint arXiv:1808.05854 (2018) [4](#)
54. Shamshad, F., Ahmed, A.: Class-specific blind deconvolutional phase retrieval under a generative prior. arXiv preprint arXiv:2002.12578 (2020) [4](#)
55. Shamshad, F., Ahmed, A.: Compressed sensing-based robust phase retrieval via deep generative priors. IEEE Sensors Journal **21**(2), 2286–2298 (2020) [4](#)
56. Shamshad, F., Hanif, A., Abbas, F., Awais, M., Ahmed, A.: Adaptive ptych: Leveraging image adaptive generative priors for subsampled fourier ptychography. In: Proceedings of the IEEE/CVF International Conference on Computer Vision Workshops. pp. 0–0 (2019) [4](#)
57. Shamshad, F., Hanif, A., Ahmed, A.: Subsampled fourier ptychography via pre-trained invertible and untrained network priors. In: NeurIPS 2019 Workshop on Solving Inverse Problems with Deep Networks (2019) [4](#)
58. Shamshad, F., Naseer, M., Nandakumar, K.: Clip2protect: Protecting facial privacy using text-guided makeup via adversarial latent search. In: Proceedings of the IEEE/CVF Conference on Computer Vision and Pattern Recognition. pp. 20595–20605 (2023) [2](#), [4](#), [9](#), [11](#)
59. Shamshad, F., Srivatsan, K., Nandakumar, K.: Evading forensic classifiers with attribute-conditioned adversarial faces. In: Proceedings of the IEEE/CVF Conference on Computer Vision and Pattern Recognition. pp. 16469–16478 (2023) [4](#)
60. Shan, S., Wenger, E., Zhang, J., Li, H., Zheng, H., Zhao, B.Y.: Fawkes: Protecting privacy against unauthorized deep learning models. In: Proceedings of the 29th USENIX Security Symposium (USENIX Security’20). pp. 1589–1604 (2020) [3](#)
61. Sharif, M., Bhagavatula, S., Bauer, L., Reiter, M.K.: A general framework for adversarial examples with objectives. ACM Transactions on Privacy and Security (TOPS) **22**(3), 1–30 (2019) [3](#)
62. Song, Y., Shu, R., Kushman, N., Ermon, S.: Constructing unrestricted adversarial examples with generative models. Advances in Neural Information Processing Systems **31** (2018) [2](#), [3](#)
63. Sun, Y., Yu, L., Xie, H., Li, J., Zhang, Y.: Diffam: Diffusion-based adversarial makeup transfer for facial privacy protection. In: Proceedings of the IEEE/CVF Conference on Computer Vision and Pattern Recognition. pp. 24584–24594 (2024) [4](#), [9](#)
64. Tov, O., Alaluf, Y., Nitzan, Y., Patashnik, O., Cohen-Or, D.: Designing an encoder for stylegan image manipulation. ACM Transactions on Graphics (TOG) **40**(4), 1–14 (2021) [20](#)
65. Tumanyan, N., Bar-Tal, O., Bagon, S., Dekel, T.: Splicing vit features for semantic appearance transfer. In: Proceedings of the IEEE/CVF Conference on Computer Vision and Pattern Recognition. pp. 10748–10757 (2022) [7](#)

66. Ulyanov, D., Vedaldi, A., Lempitsky, V.: Deep image prior. In: Proceedings of the IEEE conference on computer vision and pattern recognition. pp. 9446–9454 (2018) [4](#)
67. Wang, M., Deng, W.: Deep face recognition: A survey. *Neurocomputing* **429**, 215–244 (2021) [1](#)
68. Wang, Y., Bao, T., Ding, C., Zhu, M.: Face recognition in real-world surveillance videos with deep learning method. In: 2017 2nd international conference on image, vision and computing (icivc). pp. 239–243. IEEE (2017) [1](#)
69. Wenger, E., Shan, S., Zheng, H., Zhao, B.Y.: Sok: Anti-facial recognition technology. arXiv preprint arXiv:2112.04558 (2021) [1](#)
70. Xia, W., Zhang, Y., Yang, Y., Xue, J.H., Zhou, B., Yang, M.H.: Gan inversion: A survey. *IEEE Transactions on Pattern Analysis and Machine Intelligence* (2022) [4](#)
71. Xiao, Z., Gao, X., Fu, C., Dong, Y., Gao, W., Zhang, X., Zhou, J., Zhu, J.: Improving transferability of adversarial patches on face recognition with generative models. In: Proceedings of the IEEE/CVF Conference on Computer Vision and Pattern Recognition. pp. 11845–11854 (2021) [2](#), [3](#)
72. Yang, X., Dong, Y., Pang, T., Su, H., Zhu, J., Chen, Y., Xue, H.: Towards face encryption by generating adversarial identity masks. In: Proceedings of the 2021 IEEE/CVF International Conference on Computer Vision (ICCV’21). pp. 3897–3907 (2021) [2](#), [3](#), [9](#), [10](#), [11](#), [12](#), [20](#), [21](#)
73. Yang, X., Wei, F., Zhang, H., Zhu, J.: Design and interpretation of universal adversarial patches in face detection. In: Computer Vision–ECCV 2020: 16th European Conference, Glasgow, UK, August 23–28, 2020, Proceedings, Part XVII 16. pp. 174–191. Springer (2020) [2](#)
74. Yin, B., Wang, W., Yao, T., Guo, J., Kong, Z., Ding, S., Li, J., Liu, C.: Advmakeup: A new imperceptible and transferable attack on face recognition. In: Proceedings of the 30th International Joint Conference on Artificial Intelligence (IJCAI’21). pp. 1252–1258 (2021) [2](#), [9](#), [10](#), [11](#), [20](#)
75. Yin, B., Wang, W., Yao, T., Guo, J., Kong, Z., Ding, S., Li, J., Liu, C.: Advmakeup: A new imperceptible and transferable attack on face recognition. arXiv preprint arXiv:2105.03162 (2021) [3](#)
76. Yu, C., Wang, J., Peng, C., Gao, C., Yu, G., Sang, N.: Bisenet: Bilateral segmentation network for real-time semantic segmentation. In: Proceedings of the European conference on computer vision (ECCV). pp. 325–341 (2018) [9](#)
77. Yuan, S., Zhang, Q., Gao, L., Cheng, Y., Song, J.: Natural color fool: Towards boosting black-box unrestricted attacks. arXiv preprint arXiv:2210.02041 (2022) [2](#), [3](#)
78. Zhang, K., Zhang, Z., Li, Z., Qiao, Y.: Joint face detection and alignment using multitask cascaded convolutional networks. *IEEE signal processing letters* **23**(10), 1499–1503 (2016) [9](#), [20](#)
79. Zhao, Z., Liu, Z., Larson, M.: Towards large yet imperceptible adversarial image perturbations with perceptual color distance. In: Proceedings of the IEEE/CVF Conference on Computer Vision and Pattern Recognition. pp. 1039–1048 (2020) [2](#), [3](#)
80. Zhong, Y., Deng, W.: Opom: Customized invisible cloak towards face privacy protection. *IEEE Transactions on Pattern Analysis and Machine Intelligence* (2022) [3](#)
81. Zhu, Z.A., Lu, Y.Z., Chiang, C.K.: Generating adversarial examples by makeup attacks on face recognition. In: 2019 IEEE International Conference on Image Processing (ICIP). pp. 2516–2520. IEEE (2019) [3](#)

Supplementary: Makeup-Guided Facial Privacy Protection via Untrained Neural Network Priors

6 Datasets Description and Preprocessing

This section outlines the datasets and processing steps used in our experiments:

- **CelebA-HQ** [26]: High-resolution dataset (1024×1024) with 30,000 images. We use 1000 images of different identities as provided by Hu *et al.* [20].
- **LADN** [13]: Makeup-based dataset used for impersonation attacks in face verification. We use 332 non-makeup images split into four groups, each targeting one of four identities provided by Hu *et al.* [20].
- **LFW** [21]: Face identification dataset with 13,233 images and 5,749 identities. Used for face verification (dodging) and face identification (impersonation and dodging). We select 500 pairs, each of the same identity.

We use CelebA-HQ and LADN for impersonation attacks in face verification, and CelebA-HQ and LFW for other settings. This combination demonstrates our method’s generalization across high-quality (CelebA-HQ) and low-quality (LFW) images.

Preprocessing: We use MTCNN [78] for face detection, cropping, and alignment before input to FR models. Additional preprocessing follows Tov *et al.* [64] for latent code initialization.

7 Dodging Attack under Face Verification

Tab. 9 presents PSR results for dodging attacks in face verification under a black-box setting. We use 500 randomly selected subjects, each with a pair of faces. We compare DFPP only with the state-of-the-art noise-based method TIP-IM, as Adv-Makeup [74] and AMT-GAN [20] are designed specifically for impersonation attacks. Our method DFPP demonstrates superior performance, achieving an absolute gain of over 5% compared to TIP-IM.

Table 9: Protection success rate (PSR %) of *black-box* dodging attack under the face verification task. For each column, the other three FR systems are used as surrogates to generate the protected faces. We exclude Adv-Makeup [74] and AMT-GAN [20] as they are trained specifically for impersonation attacks.

Method	CelebA-HQ				LFW				Average
	IRSE50	IR152	FaceNet	MobileFace	IRSE50	IR152	FaceNet	MobileFace	
TIP-IM [72]	71.2	69.4	88.2	59.0	71.8	76.1	80.6	62.9	72.4
DFPP (Ours)	79.0	80.4	91.7	62.1	76.2	78.6	85.3	70.9	78.0

Table 10: Protection success rate (PSR %) of *black-box* dodging (top) and impersonation (bottom) attacks under the face identification task for CelebA-HQ dataset [21]. For each column, the other three FR systems are used as surrogates to generate the protected faces. R1-U: Rank-1-Untargeted, R5-U: Rank-5-Untargeted, R1-T: Rank-1-Targeted, R5-T: Rank-5-Targeted.

Method	IRSE50		IR152		FaceNet		MobileFace		Average	
	R1-U	R5-U								
TIP-IM [72]	79.6	61.2	62.9	42.8	46.2	27.8	81.9	76.7	67.6	52.1
Ours	85.2	68.8	67.4	45.3	54.1	29.5	91.2	81.0	74.5	56.1
Method	IRSE50		IR152		FaceNet		MobileFace		Average	
	R1-T	R5-T								
TIP-IM [72]	16.2	51.4	21.2	56.0	8.1	35.8	9.6	24.0	13.8	41.8
Ours	22.1	60.2	23.7	62.4	11.8	37.4	11.1	27.6	17.2	46.9

8 Results for Face Identification

The PSR on CelebA-HQ dataset for dodging and impersonation attacks are provided in Tab. 10. For this experiment, we randomly select 500 subjects, each having a pair of faces. We assign one image from each pair to the gallery set, and the other to the probe set. Both impersonation and dodging attacks are conducted on the probe set. We excluded AMT-GAN and Adv-Makeup from both tables, as they are specifically trained for the face verification task.

9 Results for Tencent Yunshent API

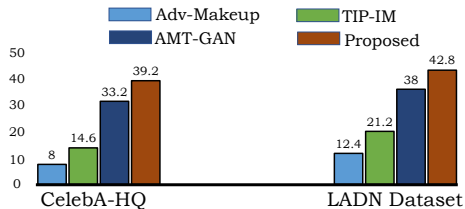


Fig. 9: Average confidence scores (where higher scores are preferable) from commercial API Tencent Yunshentu for impersonation attacks within the face verification framework. The DFPP method consistently outperforms these approaches.

We evaluate DFPP’s effectiveness against the commercial API Tencent Yunshentu, operating in verification mode for impersonation. This API returns confidence scores from 0 to 100, with higher scores indicating greater similarity between two images. As the training data and model parameters of this proprietary FR system are undisclosed, this test effectively simulates a real-world scenario. We protect 100 faces from the CelebA-HQ dataset using both baseline methods and DFPP. Fig. 9 illustrates the average confidence scores returned by



Fig. 10: Reference makeup images used by [20] to adversarially transfer makeup to the source image.

Tencent Yunshentu for these protected images. The results clearly demonstrate DFPP’s superior PSR compared to the baselines, underscoring its effectiveness in real-world applications.

10 Reference Makeup Images

In all our experiments, we utilize the reference makeup images shown in Fig. 10. These diverse images, provided by [20], represent a wide range of makeup styles, from subtle to dramatic. Our results are averaged over these ten reference images, ensuring a comprehensive evaluation of our method’s performance across various makeup styles.